

A Comparison of Machinability in Hard Turning of EN-24 Alloy Steel Under Mist Cooled and Dry Cutting Environments with a Coated Cermet Tool

Anshuman Das · Nirmal Tirkey · Saroj Kumar Patel · Sudhansu Ranjan Das ·
Bibhuti Bhusan Biswal

Submitted: 10 September 2018 / Published online: 5 December 2018
© ASM International 2018

Abstract In this current research, mist cooling and dry cutting effects on cutting force, flank wear, chip morphology, crater wear, surface roughness and microhardness of chip have been evaluated during hard turning operation of EN-24 grade steel having hardness of 48 HRC. Water-soluble oil was applied for cooling and lubricating purposes in mist cooling, and a comprehensive comparative analysis was performed with dry machining environment. Dry machining was found more effective as compared to mist cooling technique against the chip microhardness and cutting force. For other responses like crater wear, flank wear, surface roughness and chip morphology, the cooling setup having coolant delivered in mist form performed better than dry machining owing to reduction in cutting zone temperature and complimentary modification in chip-tool interaction during hard turning.

Keywords Hard turning · Mist cooling · Crater wear · Microhardness · Surface roughness · Cutting force · ANOVA · Chip morphology · Flank wear · Cermet

Introduction

In the era of tough competition, industries are constantly striving to achieve newer heights. Keeping the production cost pristine and enhancing the product quality without affecting the environment are the most focussed engineering challenge for today. Innovative solutions to manufacturing problems are implicative experimental investigations. The major shortcoming of any machining operation is heat produced and dissipation to surrounding atmosphere, especially in tool–chip–work interfaces. Though chip drives away most of the heat with it, a fraction of heat is conducted to work and cutting inserts. This heat generation phenomenon affects the machining cost adversely. To minimize the heat produced and increase the machining aspects, production industries are using various metal cutting fluids in machining operations. The cost of the metal cutting fluids and their impact to the surrounding environment are a primary concern. Hence, scientists and researchers are doing enormous research on the above issues by adopting various methods. Minimum quantity lubrication (MQL) or mist cooling can solve the above-mentioned issues. Mist cooling technique includes a small fraction of coolant in the machining zone and tries to supplant the conventional flooded cooling system. Using large volume of cutting fluids severely affects the environment and hikes machining costs. Disposal of wet chips is another chief concern. The prolonged issues are closely related to potential health risk during machining operation with the application of conventional coolant which still remains a great challenge to be worked upon.

A. Das · B. B. Biswal
Department of Industrial Design, National Institute of
Technology, Rourkela 769008, Odisha, India

N. Tirkey · S. K. Patel
Department of Mechanical Engineering, National Institute of
Technology, Rourkela 769008, Odisha, India

S. R. Das (✉)
Department of Production Engineering, Veer Surendra Sai
University of Technology, Burla 768018, Odisha, India
e-mail: das.sudhansu83@gmail.com

Literature Review

Sudheer et al. [1] studied the effects of various cutting conditions on the surface roughness in turning of aluminum metal matrix composite and revealed that MQL machining outperformed dry and compressed refrigerated air machining. Lawal et al. (2015) analyzed the effects of cutting fluids on carbide inserts flank wear during turning of AISI 4340 grade steel and found that palm kernel oil performed far better than cottonseed and mineral oil. Sanchez et al. [2] found a newer approach for cooling through tool holder during machining activity and observed that internal cooling outperformed dry machining and machining with conventional coolant supply with respect to cutting temperature, tool life and surface roughness. Alkali et al. [3] investigated the effect of cutting speed and feed on the formation of chips during turning of hardened tool steel. Both speed and feed were the most dominating parameters for chip thickness and serration found in the chips. Saini et al. [4] compared the working capabilities of PVD- and CVD-coated carbide inserts under both dry and MQL cutting conditions. The experimental outcomes unveiled that machining with MQL setup was found better than dry cutting condition and PVD-coated inserts outperformed CVD-coated inserts. Vardhaman et al. [5] also experimented on the effect of cutting liquids while machining AISI 1040 grade steel. Among the various cutting conditions, MQL with coconut oil performed better. Exorbitant flank wear and cutting force were resulted in the dry and wet cutting environments as compared to other setups. Elmunafi et al. [6] delineated that tool life can be enhanced for carbide tool coated with MQL technique adding castor oil while machining of hardened stainless steel. From ANOVA analysis, it was made clear that speed was the most significant parameter for tool life as than to feed. Stephenson et al. [7] made a comparative analysis among CO₂-based MQL and water-based flood cooling while executing rough machining of Inconel 750. They observed that higher tool life and MRR were obtained with CO₂-based MQL than water-based flood cooling. Bose et al. [8] conducted machining on Nicrofer C263 with various cutting environments, and outcomes were compared. Minimum values of various machining attributes were produced during machining with MQL having 4% Al₂O₃ nanoparticles. Krishna et al. [9] also examined the nanoboric particles performance with SAE-40 and coconut oil while machining AISI 1040 steel. Outcomes proved that the overall performance of nanoparticle-based coconut oil was found better than SAE-40 fluid. Netake and Chinchankar [10] exhibited a scientific model on hard turning utilizing MQL technique. Feed and depth of cut were the most dominating parameters affecting the responses compared to the cutting velocity. Goindi et al. [11] investigated

the ionic liquid performance while conducting machining of AISI 1045 steel, and results were compared with other cutting conditions. From the results, they deduced that MQL with ionic liquid performed better among all other machining environments. Sharma and Dixit [12] analyzed two distinct cutting environments in turning of gray cast iron with mixed ceramic tool. From the research, they presumed that air cooled turning was better to dry turning of cast iron. Ezugwu et al. [13] did machining operation on Inconel 718 with ceramic inserts under various coolant pressures. High coolant pressure was an advantage for machining forces, chip segmentations and roughness, whereas it was not effective for better tool life. Khan et al. [14] compared the effects of three cutting environments during turning of 9310 alloy steel. They observed that MQL machining was dominant on dry and wet machining for various responses. Ojolo et al. [15] evaluated the outcomes of various biological oils on cutting force and coefficient of friction during turning of different workpieces. The results declared that biological oils were the best choices for cutting fluids during machining. Dhar et al. [16] differentiated the effects of distinctive cutting environments on various results in turning of AISI 1040 steel. The results demonstrated that MQL's performance was more persuasive on the output responses than dry and wet cutting environments. Diniz et al. [17] performed experiments at different cutting speeds on 52100 hardened steel using CBN tools with various cutting environments. The authors claimed that dry cutting environment performed better than both wet and minimum volume of oil cutting conditions. Gill et al. [18] analyzed the wear of cryogenically treated inserts during continuous and interrupted turning under dry and wet cutting conditions. Results illustrated that cryo-treated inserts were steady in interrupted turning as compared to continuous turning with dry and wet cutting environments. Attanasio et al. [19] did a comparative analysis on the tool life in two different cutting environments in which it was found that the MQL's performance was superior to dry machining. Cakir et al. [20] analyzed the effects of various gases in turning, and outcomes were compared against dry and wet cutting environments. Performance of turning in the gaseous environment was found better relative to dry and wet machining environments in the outcomes. Selopal and Bhatia [21] reviewed various research articles on machining operations using coolant and suggested that coolant supplied to machining zones with MQL setup is a finer alternative than dry and flood cooling conditions. Surface roughness was analyzed while machining of EN-31 steel in different cutting conditions by Singh et al. [22]. The results showed that MQL with vegetable oil produced least roughness by magnitude as compared to other two cutting conditions. Maruda et al. [23] analyzed the tool wear

mechanisms in turning with three different cutting conditions. MQCL (minimum quantity cooling and lubrication) with phosphate ester-based additive produced enhanced tool life compared to other two cutting environments. Cutting tool wear and chip formation mechanism were studied by Maruda et al. [24] under three cutting environments. Better chip morphology and less tool wear were found during machining operation with MQCL with phosphate ester enriched additive compared to other cutting conditions. Maruda and Feldshtein [25] studied various chip characteristics and surface roughness in finish turning of low carbon steel. Outcomes are put in comparison for three cutting conditions. The best alternative was found in MQCL environment. Maruda et al. [26] made a comparative analysis on surface roughness while doing turning under different MQCL conditions. Least roughness was observed for MQCL with anti-wear additive than other cutting environments. Maruda et al. [27] performed machining operation under three cutting conditions. Results delineated that superior chip morphology and roughness were observed for MQL and MQCL conditions compared to dry cutting condition.

From the literature review, it was made clear that CBN, ceramic and carbide cutting inserts have been used extensively by various researchers. However, significant studies have not been carried out with cermet insert. A little work has been executed on the impact of machining attributes and cutting conditions on chip morphology and micro-hardness which is an important machining attribute. In addition to that, different cutting fluids such as castor oil, vegetable oils, nanofluid and ionic fluid have been used by many researchers. However, the impacts of soluble coolant have not been investigated adequately. Furthermore, it was unveiled that in most of the cases, flank wear, surface roughness, heat-affected zone temperature and machining forces have been considered as dominant machining properties, but the crater wear has not been recognized as an important machining attribute.

The core objective of the current work focuses on the comparative assessment of various machinability attributes using multilayer coated cermet inserts in hard turning of EN-24 alloy steel with a hardness of 48 HRC under both mist and dry cooling environments with a water-soluble coolant.

Experimental Methods

The test specimen is a cylindrical workpiece of EN-24 alloy steel having diameter 40 mm and length 500 mm with hardness of 48 HRC used under dry and mist cooling setups. Figure 1 shows the experimental setup. Three machining factors such as cutting speed, feed and depth of

cut are chosen for the current study. Trial runs are executed as per Taguchi’s L_9 orthogonal array to save both time span and production cost when compared to a full factorial configuration without disturbing precision of the results. Table 1 shows the experimental layout of Taguchi’s L_9 orthogonal array, and Table 2 shows the chemical composition of the work material.

The exterior layers were initially removed from the outer surface of the workpiece before conducting the machining operation to relieve any outcome of non-consistency on the outcomes. The machining strategy for both the cutting environments is shown in Table 3. Triplicate experiments were performed for each combination of speed, feed and depth of cut for each response, and their mean value was considered as final to keep the experimental error in check. The cutting force measurement was accomplished using Kistler three-dimensional stationary dynamometer and charge amplifier. The newer cutting edge of the insert was set for different trial runs. After each such trial, flank wear and crater wear of the insert were analyzed

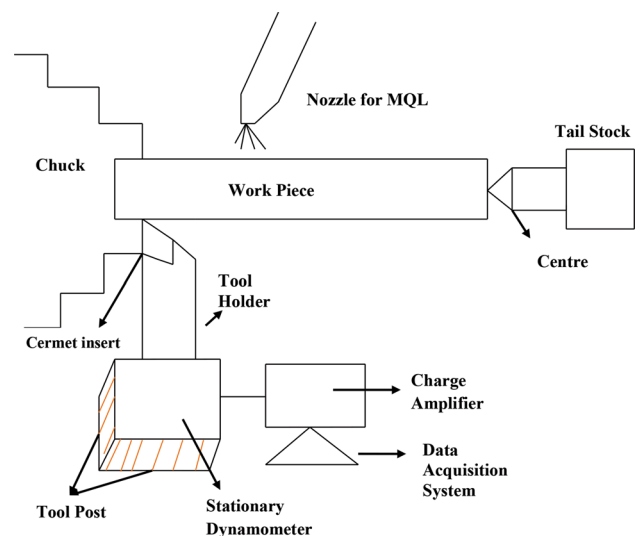


Fig. 1 Experimental layout with force measurement setup

Table 1 Experimental layout of Taguchi’s L_9 orthogonal array

| Experiment no. | Speed | Feed | Depth of cut |
|----------------|-------|------|--------------|
| 1 | 1 | 1 | 1 |
| 2 | 1 | 2 | 2 |
| 3 | 1 | 3 | 3 |
| 4 | 2 | 1 | 2 |
| 5 | 2 | 2 | 3 |
| 6 | 2 | 3 | 1 |
| 7 | 3 | 1 | 3 |
| 8 | 3 | 2 | 1 |
| 9 | 3 | 3 | 2 |

using scanning electron and advanced optical microscope. Chips were collected, and the morphological analysis was performed out after each run with the help of SEM. Chip microhardness was measured using Vickers microhardness tester after mounting and polishing of chip samples with polishing papers of different grades. Three readings were noted for each response, and their mean value was specified as the final. Water-soluble coolant was supplied at 150 ml/h and at a pressure of 7 bar. The coolant was prepared with a ratio of 10:1. Figure 2 shows the complete setup for cutting fluid supply with MQL technique where both the coolant and pressurized air were mixed and supplied to the machining zone through the nozzle.

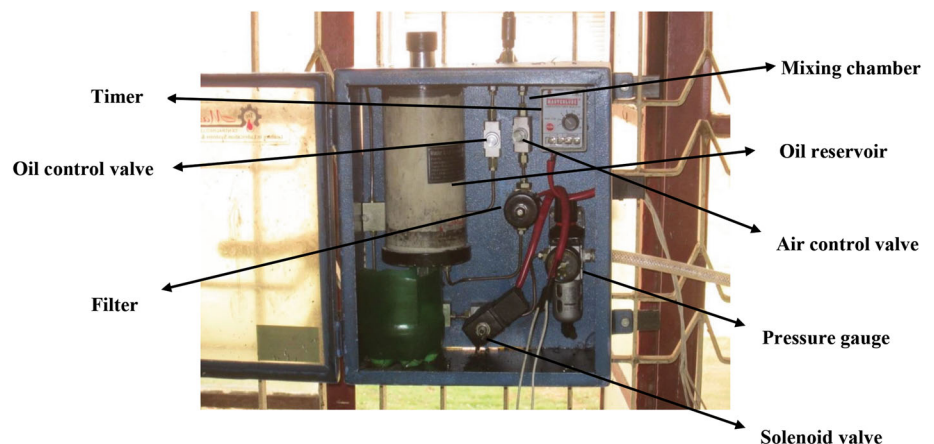
Table 2 Weight percentage of various constituents in EN-24 steel

| Elements | Weight percentage |
|------------|-------------------|
| Carbon | 0.402 |
| Silicon | 0.340 |
| Manganese | 0.770 |
| Nickel | 1.551 |
| Chromium | 0.900 |
| Molybdenum | 0.276 |
| Iron | 95.61 |

Table 3 Machining condition

| Machining conditions | Descriptions |
|----------------------|---------------------------|
| Cutting speed | 80, 100, 120 m/min |
| Feed rate | 0.05, 0.1, 0.15 mm/rev |
| Depth of cut | 0.1, 0.2, 0.3 mm |
| Cutting environment | Dry cutting, mist cooling |
| Machining length | 250 mm |

Fig. 2 Setup for cutting fluid supply with MQL technique



Cutting Tool and Tool Holder

Cermet inserts utilized in this investigation were multilayer (TiN/TiCN/TiN) PVD coated with designation CNMG 120408 outlined by grade KT315ff from Kennametal of rhombic structure (80° point, angle) with finished chip breaker geometry. The tool holder used to mount the inserts designated by PCLNR 2020K12 with clearance angle = 0° , back and side rake angle = -6° , entering angle = 95° , point angle = 80° and nose radius = 0.8 mm.

Results and Discussion

The results produced from the experiments for coated cermet in mist and dry cooling conditions are shown in Tables 4 and 5, respectively. These tables exhibit the observations of cutting force F_z , flank wear VB_c , crater wear width K_w , surface roughness R_a and microhardness of the chip for nine runs.

ANOVA (Analysis of Variance)

Variance analysis was executed for both mist and dry cooling setups to measure significance levels of input parameters on various output attributes. In every ANOVA table, R -Sq and R -Sq (adj) values were considered to check the data fitment with the standard model. Each ANOVA table was made with a significance level of 5%. The R -Sq values determine the rate of variety in a dependent variable categorized by its inclusion with one or more independent variables, whereas R -Sq (adj) provides variety rate classified by only those independent factors that as a general rule affects the dependent parameter.

Table 6 exhibits outcomes of ANOVA for cutting force in mist cooling environment. P values illustrated the importance of input variables on the output parameters. The contribution fraction was defined as the importance of

Table 4 Experimental results using coated cermet with dry cutting

| Run no. | v (m/min) | f (mm/rev) | d (mm) | F_z (N) | VBc (mm) | K_w (mm) | Microhardness (HV) | Surface roughness, Ra (μm) |
|---------|-------------|--------------|----------|-----------|----------|------------|--------------------|---|
| 1 | 80 | 0.05 | 0.1 | 104 | 0.18932 | 0.29341 | 280 | 1.20 |
| 2 | 80 | 0.10 | 0.2 | 118 | 0.12932 | 0.24437 | 420 | 1.29 |
| 3 | 80 | 0.15 | 0.3 | 159 | 0.11223 | 0.18621 | 519 | 1.34 |
| 4 | 100 | 0.05 | 0.2 | 99 | 0.13996 | 0.24753 | 395 | 1.60 |
| 5 | 100 | 0.10 | 0.3 | 123 | 0.05178 | 0.18762 | 530 | 1.67 |
| 6 | 100 | 0.15 | 0.1 | 76 | 0.08036 | 0.23672 | 452 | 1.82 |
| 7 | 120 | 0.05 | 0.3 | 119 | 0.16833 | 0.19902 | 458 | 2.10 |
| 8 | 120 | 0.10 | 0.1 | 71 | 0.11132 | 0.26390 | 416 | 2.39 |
| 9 | 120 | 0.15 | 0.2 | 88 | 0.13894 | 0.19832 | 516 | 2.61 |

Table 5 Experimental results using coated cermet with mist cooling

| Run no. | v (m/min) | f (mm/rev) | d (mm) | F_z (N) | VBc (mm) | K_w (mm) | Microhardness (HV) | Surface roughness, Ra (μm) |
|---------|-------------|--------------|----------|-----------|----------|------------|--------------------|---|
| 1 | 80 | 0.05 | 0.1 | 77 | 0.06814 | 0.14217 | 401 | 0.623 |
| 2 | 80 | 0.10 | 0.2 | 110 | 0.12256 | 0.19832 | 557 | 0.649 |
| 3 | 80 | 0.15 | 0.3 | 162 | 0.07631 | 0.13834 | 521 | 0.686 |
| 4 | 100 | 0.05 | 0.2 | 108 | 0.13032 | 0.17825 | 478 | 0.702 |
| 5 | 100 | 0.10 | 0.3 | 139 | 0.04929 | 0.17279 | 630 | 0.713 |
| 6 | 100 | 0.15 | 0.1 | 126 | 0.07321 | 0.11934 | 518 | 0.733 |
| 7 | 120 | 0.05 | 0.3 | 134 | 0.15132 | 0.10032 | 495 | 0.741 |
| 8 | 120 | 0.10 | 0.1 | 111 | 0.10763 | 0.11416 | 575 | 0.749 |
| 9 | 120 | 0.15 | 0.2 | 154 | 0.12821 | 0.10422 | 541 | 0.755 |

Table 6 ANOVA of cutting force for cermet with mist cooling

| Source | DF | SS | MS | F | P | Percentage contribution (p) |
|-------------|----|------------------------|---------|----------------------------------|-------|-----------------------------|
| v | 2 | 416.89 | 208.44 | 15.50 | 0.061 | 7.57 |
| f | 2 | 2614.89 | 1307.44 | 97.25 | 0.010 | 47.54 |
| d | 2 | 2441.56 | 1220.78 | 90.80 | 0.011 | 44.39 |
| Error | 2 | 26.89 | 13.44 | – | – | 0.48 |
| Total | 8 | 5500.22 | – | – | – | 100 |
| $S = 3.667$ | – | $R\text{-Sq} = 99.5\%$ | – | $R\text{-Sq}(\text{adj}) = 98\%$ | – | – |

the machining parameters on the cutting force. Among all factors, feed had the highest significance on cutting force with a percentage contribution of 47.54% and depth of cut was the second most significant factor with a contribution of 44.39%. The cutting speed was observed to have no prominent effect on cutting force. Table 7 unveils ANOVA results for cutting force during dry hard turning of EN-24 steel using cermet inserts. Factors like speed and depth of cut were observed to be statistically important for cutting force, but feed was not important. The percentage contributions of three machining parameters, i.e., speed, feed and depth of cut, are 33.80, 0.66 and 65.00%, respectively. Thus, depth of cut was the most prominent factor that influenced the cutting force in dry machining.

Similarly, ANOVA results of flank wear are shown in Table 8. Depth of cut, feed and cutting speed contributed for flank wear, respectively, 36.04, 32.84 and 30.49%. All the three input variables were found to essential for flank wear. The ANOVA results of flank wear shown in Table 9 were for dry cutting environment. All the three input factors were observed to be prominent with contributions, respectively, of 36.18, 56.39 and 7.39%. However, feed had the highest contribution for cermet flank wear.

Table 10 illustrates ANOVA results of crater wear for cutting inserts in mist cooling with considerable $R\text{-Sq}$ values. It was made clear that cutting speed and feed influenced inserts crater wear most significantly compared to depth of cut, which had a small contribution of 19.25%.

Table 7 ANOVA of cutting force for cermet with dry cutting

| Source | DF | SS | MS | <i>F</i> | <i>P</i> | Percentage contribution (p) |
|------------------|----|----------------------|---------|---------------------------|----------|-----------------------------|
| <i>v</i> | 2 | 2072.67 | 1036.33 | 63.45 | 0.016 | 33.80 |
| <i>f</i> | 2 | 40.67 | 20.33 | 1.24 | 0.445 | 0.66 |
| <i>d</i> | 2 | 3986.00 | 1993.00 | 122.02 | 0.008 | 65.00 |
| Error | 2 | 32.67 | 16.33 | – | – | 0.53 |
| Total | 8 | 6132.00 | – | – | – | 100 |
| <i>S</i> = 4.041 | – | <i>R</i> -Sq = 99.5% | – | <i>R</i> -Sq(adj) = 97.9% | – | – |

Table 8 ANOVA of flank wear for cermet with mist cooling

| Source | DF | SS | MS | <i>F</i> | <i>P</i> | Percentage contribution (p) |
|---------------------|----|----------------------|----------|---------------------------|----------|-----------------------------|
| <i>v</i> | 2 | 0.004381 | 0.002191 | 50.71 | 0.019 | 30.49 |
| <i>f</i> | 2 | 0.004718 | 0.002359 | 54.61 | 0.018 | 32.84 |
| <i>d</i> | 2 | 0.005177 | 0.002589 | 59.92 | 0.016 | 36.04 |
| Error | 2 | 0.000086 | 0.000043 | – | – | 0.59 |
| Total | 8 | 0.014364 | – | – | – | 100 |
| <i>S</i> = 0.006573 | – | <i>R</i> -Sq = 99.4% | – | <i>R</i> -Sq(adj) = 97.6% | – | – |

Table 9 ANOVA of flank wear for cermet with dry cutting

| Source | DF | SS | MS | <i>F</i> | <i>P</i> | Percentage contribution (p) |
|---------------------|----|---------------------|----------|---------------------------|----------|-----------------------------|
| <i>v</i> | 2 | 0.005167 | 0.002584 | 1213.19 | 0.001 | 36.18 |
| <i>f</i> | 2 | 0.008052 | 0.004026 | 1890.47 | 0.001 | 56.39 |
| <i>d</i> | 2 | 0.001056 | 0.000528 | 247.86 | 0.004 | 7.39 |
| Error | 2 | 0.000004 | 0.000002 | – | – | 0.02 |
| Total | 8 | 0.014279 | – | – | – | 100 |
| <i>S</i> = 0.001459 | – | <i>R</i> -Sq = 100% | – | <i>R</i> -Sq(adj) = 99.9% | – | – |

Table 10 ANOVA of crater wear for cermet with mist cooling

| Source | DF | SS | MS | <i>F</i> | <i>P</i> | Percentage contribution (p) |
|---------------------|----|----------------------|----------|---------------------------|----------|-----------------------------|
| <i>v</i> | 2 | 0.005414 | 0.002707 | 163.12 | 0.006 | 54.74 |
| <i>f</i> | 2 | 0.002538 | 0.001269 | 76.47 | 0.013 | 25.66 |
| <i>d</i> | 2 | 0.001904 | 0.000952 | 57.37 | 0.017 | 19.25 |
| Error | 2 | 0.000033 | 0.000017 | – | – | 0.33 |
| Total | 8 | 0.009890 | – | – | – | 100 |
| <i>S</i> = 0.004074 | – | <i>R</i> -Sq = 99.7% | – | <i>R</i> -Sq(adj) = 98.7% | – | – |

The fraction of speed and feed was, respectively, 54.74% and 25.66%. Similarly, Table 11 shows that cermet crater wear in dry cutting environments was prominently affected by feed and depth of cut as their *P* values were less than 0.05. Depth of cut had the highest dominance with a contribution of 71.68% among all inputs, followed by feed having the contribution of 21.07%. Cutting speed was found less dominant for crater wear while using dry cutting environment.

Table 12 describes the ANOVA results for chip microhardness. Feed had the maximum significance and depth of cut had the minimum contribution among three input variables for chip microhardness. Table 13 depicts ANOVA for chip microhardness during hard machining of EN-24 steel utilizing cermet inserts under dry cutting environment. All three machining input variables had prominent influences on the chip microhardness. The fraction of feed had maximum of 43.94% as compared to

Table 11 ANOVA of crater wear for cermet with dry cutting

| Source | DF | SS | MS | <i>F</i> | <i>P</i> | Percentage contribution (p) |
|---------------------|----|----------------------|----------|---------------------------|----------|-----------------------------|
| <i>v</i> | 2 | 0.000752 | 0.000376 | 10.54 | 0.087 | 6.60 |
| <i>f</i> | 2 | 0.002400 | 0.001200 | 33.67 | 0.029 | 21.07 |
| <i>d</i> | 2 | 0.008163 | 0.004082 | 114.50 | 0.009 | 71.68 |
| Error | 2 | 0.000071 | 0.000036 | – | – | 0.62 |
| Total | 8 | 0.011387 | – | – | – | 100 |
| <i>S</i> = 0.005971 | – | <i>R</i> -Sq = 99.4% | – | <i>R</i> -Sq(adj) = 97.5% | – | – |

Table 12 ANOVA of chip microhardness for cermet with mist cooling

| Source | DF | SS | MS | <i>F</i> | <i>P</i> | Percentage contribution (p) |
|------------------|----|---------------------|----------|--------------------------|----------|-----------------------------|
| <i>v</i> | 2 | 4362.0 | 2181.0 | 1635.75 | 0.001 | 13.10 |
| <i>f</i> | 2 | 25,122.7 | 12,561.3 | 9421.00 | 0.000 | 75.33 |
| <i>d</i> | 2 | 3858.7 | 1929.3 | 1447.00 | 0.001 | 11.58 |
| Error | 2 | 2.7 | 1.3 | – | – | 0.00809 |
| Total | 8 | 33346.0 | – | – | – | 100 |
| <i>S</i> = 1.155 | – | <i>R</i> -Sq = 100% | – | <i>R</i> -Sq(adj) = 100% | – | – |

Table 13 ANOVA of chip microhardness for cermet with dry cutting

| Source | DF | SS | MS | <i>F</i> | <i>P</i> | Percentage contribution (p) |
|------------------|----|---------------------|----------|--------------------------|----------|-----------------------------|
| <i>v</i> | 2 | 6041.6 | 3020.8 | 1699.19 | 0.001 | 12.30 |
| <i>f</i> | 2 | 21,582.9 | 10,791.4 | 6070.19 | 0.000 | 43.94 |
| <i>d</i> | 2 | 21,482.9 | 10,741.4 | 6042.06 | 0.000 | 43.74 |
| Error | 2 | 3.6 | 1.8 | – | – | 0.0074 |
| Total | 8 | 49,110.9 | – | – | – | 100 |
| <i>S</i> = 1.333 | – | <i>R</i> -Sq = 100% | – | <i>R</i> -Sq(adj) = 100% | – | – |

Table 14 ANOVA of surface roughness for cermet with mist cooling

| Source | DF | SS | MS | <i>F</i> | <i>P</i> | Percentage contribution (p) |
|--------------------|----|----------------------|----------|---------------------------|----------|-----------------------------|
| <i>v</i> | 2 | 0.014209 | 0.007104 | 38.33 | 0.025 | 84.54 |
| <i>f</i> | 2 | 0.001962 | 0.000981 | 5.29 | 0.159 | 11.66 |
| <i>d</i> | 2 | 0.000265 | 0.000132 | 0.71 | 0.583 | 1.57 |
| Error | 2 | 0.000371 | 0.000185 | – | – | 2.20 |
| Total | 8 | 0.016806 | – | – | – | 100 |
| <i>S</i> = 0.01361 | – | <i>R</i> -Sq = 97.8% | – | <i>R</i> -Sq(adj) = 91.2% | – | – |

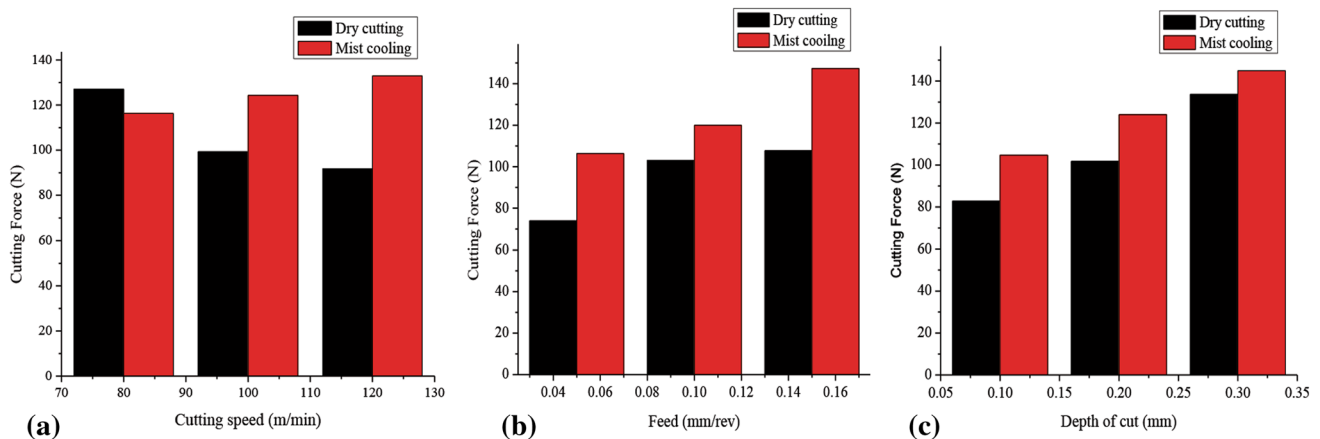
depth of cut (43.74%) and speed (12.30%) which are less significant. Speed was found as the only significant parameter for analyzing surface roughness as observed from the ANOVA (Tables 14 and 15). It had the contribution of 84.54 and 91.6% for mist cooling and dry cutting conditions, respectively.

Analysis on Cutting Force

Assessment of machining forces is crucial for machinability aspects of any material. Cutting force is generally considered as a controlling parameter for any machining process. It is the most deciding factor to judge various

Table 15 ANOVA of surface roughness for cermet with dry cutting

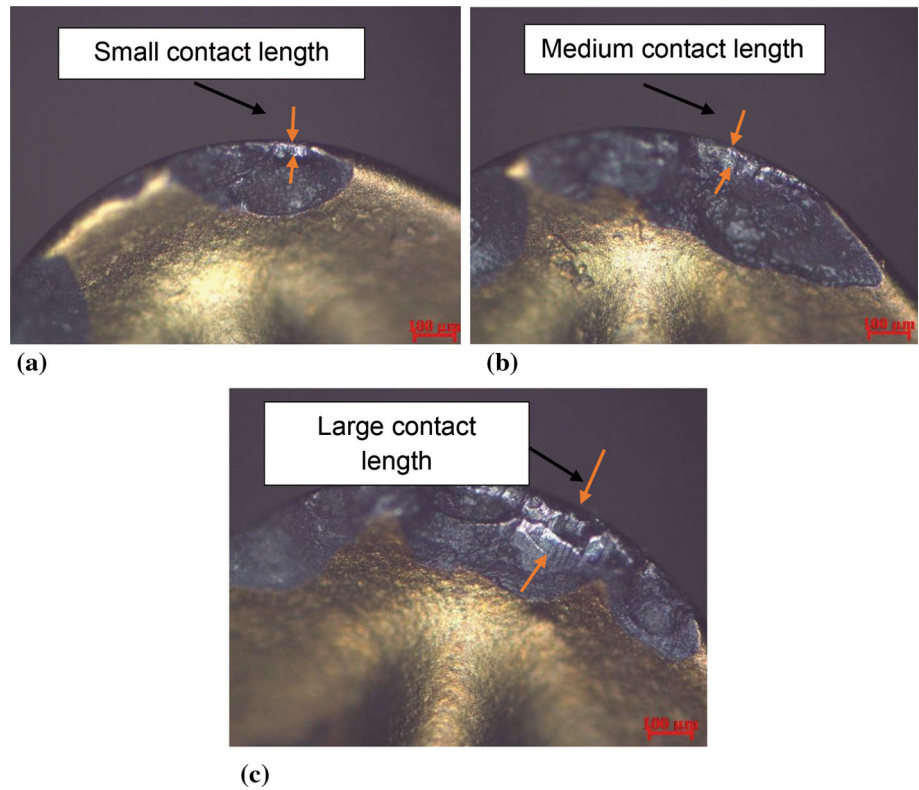
| Source | DF | SS | MS | <i>F</i> | <i>P</i> | Percentage contribution (p) |
|--------------------|----|----------------------|----------|---------------------------|----------|-----------------------------|
| <i>v</i> | 2 | 1.81340 | 0.906700 | 148.64 | 0.007 | 91.60 |
| <i>f</i> | 2 | 0.12620 | 0.063100 | 10.34 | 0.088 | 6.37 |
| <i>d</i> | 2 | 0.02780 | 0.013900 | 2.28 | 0.305 | 1.40 |
| Error | 2 | 0.01220 | 0.006100 | – | – | 0.61 |
| Total | 8 | 1.97960 | – | – | – | 100 |
| <i>S</i> = 0.07810 | – | <i>R</i> -Sq = 99.4% | – | <i>R</i> -Sq(adj) = 97.5% | – | – |

**Fig. 3** Comparison of cutting force with speed, feed and depth of cut in both cutting conditions, respectively

damages occurred on the tool and workpiece because it controls various output responses like thermal aspects in machining, dimensional deviations, deformation characteristics of workpiece and tool, surface finish, tool life and chip formation. From Fig. 3a, it was observed that cutting force reduced by enhancement of cutting speed from 80 to 100 m/min in the dry cutting environment and again diminished when speed altered to 120 m/min. Due to higher cutting speed, machining temperature escalated and it resulted in thermal softening of the specimen, which reduced the cutting forces. As tool penetrates, the work piece deforms in both primary and secondary zones due to development of compressive stresses. Moreover, this deformation helps machine energy being transformed to heat energy. The transfer of heat energy through tool–chip friction and tool–work friction results in high temperature at tool–chip interface. As discussed earlier during high-speed machining, thermal softening occurred, and because of thermal softening, grain boundary gets dislocated by which cutting force diminished. As speed increased, shear strength of the specimen decreased resulting in reduced cutting force. This was another effect of higher cutting speed on cutting force. The formations of thinner chips were observed at higher cutting speed by which the contact area between tool and chip was reduced. As a result, the strain on chip surface diminished because of which deformation was easier and cutting force was less. It was

confirmed from the above figure that higher cutting force was attained in mist cooling instead of dry cutting. Feed influenced the cutting force much more than speed and depth of cut as observed from ANOVA analysis. In the initial stage, when feed was less, the contact length between tool tip and the specimen was less, so sharpness of the insert was retained, and machining was smooth. However, as feed increased, contact length also increased as shown in Fig. 4a, b, and c. The average contact length for different levels of feed such as 0.05, 0.1 and 0.15 mm/rev was determined as 129.20 microns, 170.43 microns and 183.28 microns, respectively. So due to the enhancement of contact length at higher feed level, the sharpness of the insert reduced and machining was rough by which higher cutting force was obtained irrespective of the mist cooling environment. As discussed earlier, feed was the governing parameter for cutting force in mist cooling. This is mainly due to high material removal rate per revolution, for which more energy was consumed and higher force was generated. One more impact of feed on cutting force, cutting force increased with increased feed because of the enlargement of sheared chip area and enhancement of resistance toward the shear deformation for the specimen. From Fig. 3c, it was noticed that there was an enhancement of cutting force with the depth of cut. Many factors were responsible for the enhancement of cutting force. Due to the increase in depth of cut, roughing was more resulting in

Fig. 4 (a, b and c) Contact lengths on rake surfaces of the inserts during mist cooled turning at 0.05, 0.1 and 0.15 mm/rev feed levels



occurrence of thermal softening at the insert’s cutting edge. As a result, more force was produced in dry cutting as a result. The shear plane area was increased due to depth of cut for which more energy was consumed during machining, so higher force was generated. Also with high depth of cut, chip thickness was increased and high material removal rate was achieved for which higher cutting force was produced. From Fig. 3a, b, and c, it was concluded that higher cutting force was observed in mist cooling compared to dry cutting with speed, feed and depth of cut, because in mist cooling environment, surface hardening occurred due to rapid cooling, which is shown in Fig. 6. It is observed that chip microhardness was more compared to dry cutting due to the surface hardness enhancement of workpiece in mist cooling. Force increased in mist cooling due to more hardness.

Flank Wear Study

Abrasion was the main mechanism of flank wear in cermet inserts. It was mainly due to the hardened and martensitic structures present in the specimen shown in Fig. 5. Flank wear occurred on the flank face of the inserts when abrasion took place between the flank surface and newly generated machined surface. In the present research, hardened steel with hardness value 48 HRC was used. It was tough to machine such a hardened material because of

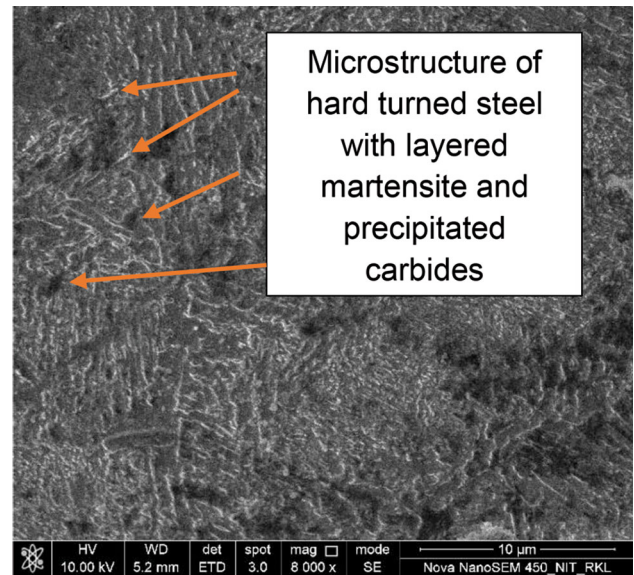


Fig. 5 Microstructure of hard turned steel sample

small carbides present at the microstructural level also indicated in Fig. 7. Additionally, thermal conductivity was reduced due to hardening; hence, heat dissipation was difficult during machining which imposed a thermal load on the inserts by which softening occurred near the cutting edge and tool wear comparatively increased. Chipping occurred at the cutting edges of the inserts mainly due to

the brittleness of the workpiece and tool material. Moreover, this was also due to high temperature and stress occurred during machining in dry cutting circumstances. Experiments conducted in this paper are of continuous type. High temperature was generated during dry turning in different cutting zones, but in mist cooling condition due to proper cooling and lubrication temperature was reduced and producing less tool wear [7, 8, 14, 19, 23]. The surface morphology at the flank surface of cermet inserts under both cutting environments is shown in Fig. 6a and b. It is observed that abrasion, adhesion, chipping and deformation were the main mechanisms of flank wear of the inserts during dry cutting condition. But in the mist cooling method, only smooth abrasion marks were observed due to diminishing temperature at the cutting zone.

Crater Wear Analysis

To study the crater wear and check the effectiveness of mist cooling process, rake surfaces of the inserts were analyzed using optical and scanning electron microscopy. On the rake surface of the inserts, crater wear was found for both the cutting conditions. In this segment, the abasement of the rake surface for the inserts has been examined while machining hardened alloy steel. Various characteristics were involved in the above analysis like properties of the

work piece and tool material, machining environments and machining parameters. The width of crater wear of the inserts has been analyzed with the help of advanced optical microscope. The width of the crater wear on the rake faces appears in Fig. 7a and b. Severe crater wear with thick chip sliding marks was observed in dry cutting, whereas crater wear with smooth sliding marks was observed in mist cooling. Crater wear was generally enhanced due to the chemical affinity between the insert and workpiece. Crater wear was not generally influenced by the hardness and toughness of the tool material. Due to the strong chemical bonding in the alloy steel, diffusion occurred at the tool–chip interface. It was very usual that due to lower thermal conductivity and extensive work hardening of hardened steel material, high temperature was generated at various machining zones and this temperature generation was one of the most powerful factors for the formation of crater wear on the rake faces of the inserts. With the advancement of machining operation, crater wear was formed on the tool rake face due to continuous interaction and rubbing of chips with workpiece and insert surface. It was formed at a marginal distance from the tool tip as shown in microscopic images discussed above. From Fig. 8a, it is evident that small pieces of chips adhered to the insert's rake face and the cutting edge was chipped off. However, neither the adhering of chips and nor the inner chip notch was noticed

Fig. 6 (a) and (b) Flank wear of insert during mist cooling and dry turning

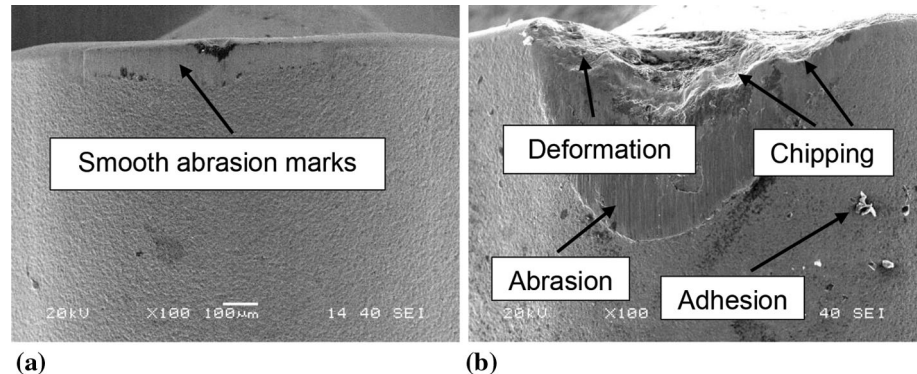


Fig. 7 (a) and (b) Crater wear of insert during dry turning and mist cooling

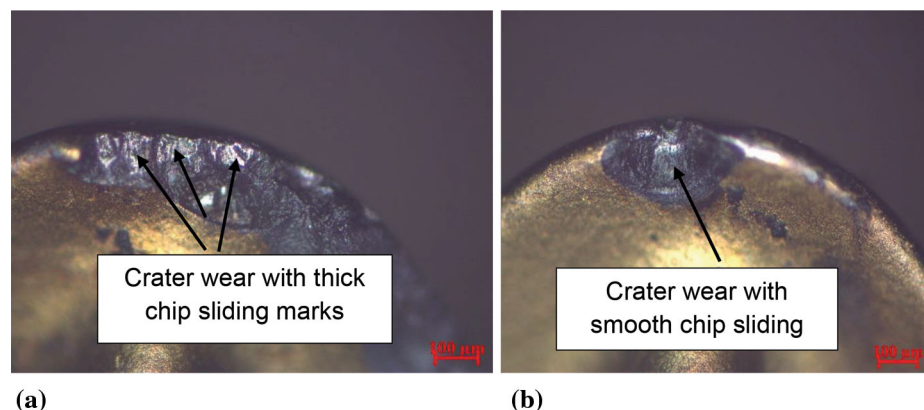


Fig. 8 (a) and (b) Rake surfaces morphology of the insert during dry cutting

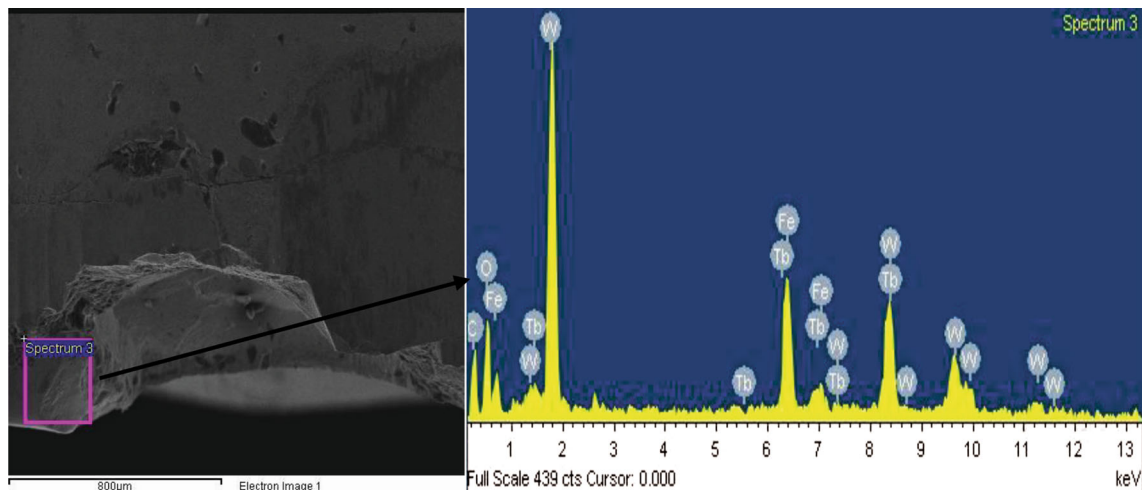
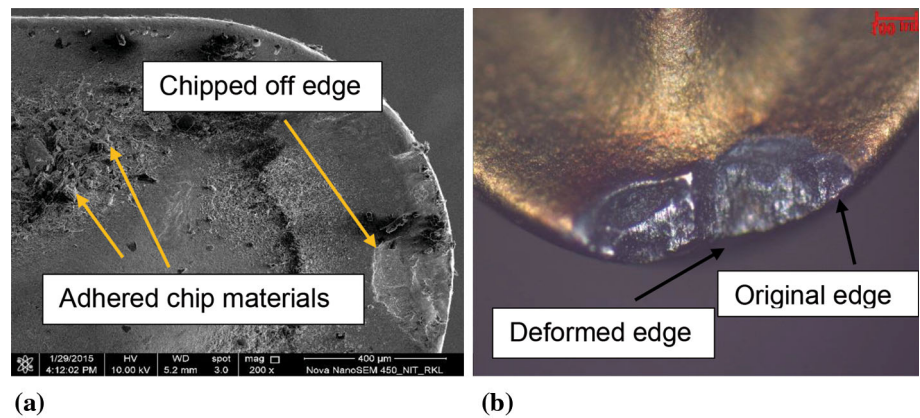


Fig. 9 SEM image with EDS spectrum for cermet after machining

during the machining of hardened steel in mist cooling environment and this appearance in mist cooling condition was due to the decrease in chip temperature. The additional cooling effect of coolant averted the softening of the chips and its sticking on the rake surfaces. The formation of crater wear on the rake surfaces of the inserts was mostly dominated by chemical reaction and thermal load as discussed earlier. The plastic deformation at the nose part of the insert occurred because of the pressure built up at the tool–chip interface. The pressure built up due to compressive stress which was developed due to high temperature in dry cutting as shown in Fig. 8b. Finally, it is concluded that crater wear was formed on the rake faces due to adhesion and diffusion. The adhesion and slippage of chips on the rake surface formed a crater. At the time of sticking of chips, the binder material of cermet inserts was damaged and removal of a small portion from the rake face was due to the breakage of chips. The wear rate on the rake face for cermet insert was higher due to diffusion. It is dependent on temperature. Diffusion was the prime reason of crater wear. From Fig. 9, it was apparent that transfer of

material from test specimen to the tool rake face occurred notably in dry machining due to high chemical affinity and thermal effects. The same material transfer from tool to workpiece is also reflected in Fig. 10.

Analysis of Chip Morphology and Microhardness

During hard turning, cutting edges of the insert were subjected to high compression and then deformed permanently. A high shear zone is formed between the contact of the workpiece and cutting inserts. Chip morphology provides vital information regarding the machining operation, because it incorporates various properties of the workpiece like mechanical, thermal and thermo-viscoelastic. There is a connection emerging between chip morphology and machining forces. The diminishing impact of machining forces occurs due to serrated chips. As shown in Fig. 11, there was a continuous serration on the chip surface in dry cutting condition. However, chip with least serration was observed in mist cooling explained (Fig. 12). Between the two successive

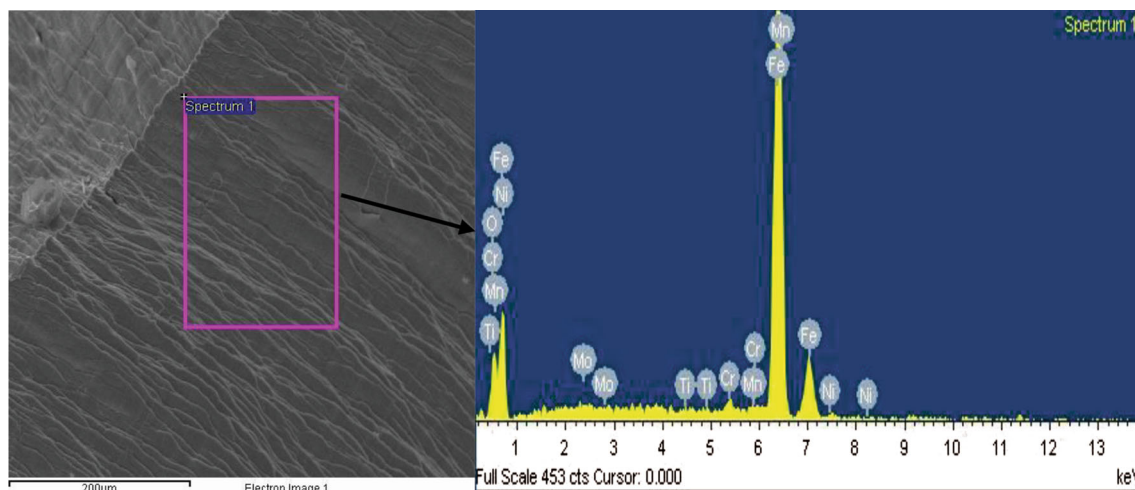


Fig. 10 SEM image with EDS spectrum for cutting chips after machining

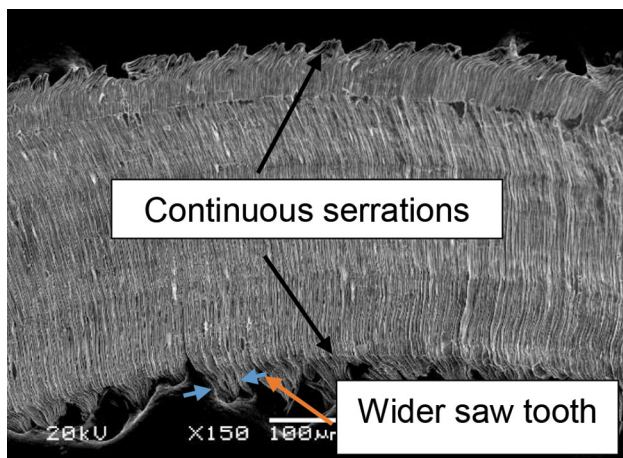


Fig. 11 Chip with dry cutting

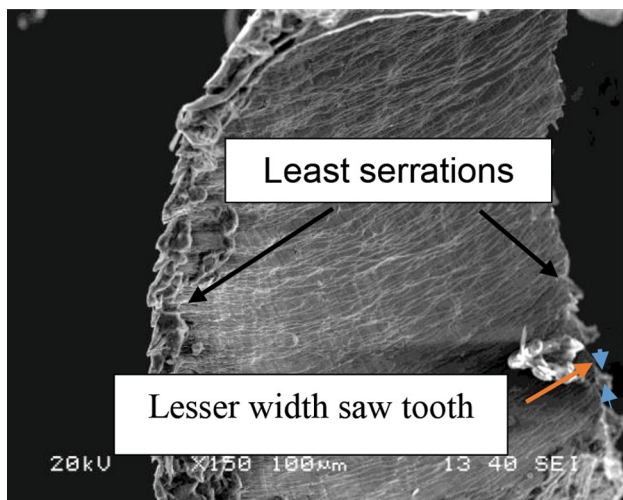


Fig. 12 Chip with mist cooling

serrations or saw tooth of the chip, permanent deformation is profound. This deformation is confined in a narrow region. This narrow region is called the adiabatic shear band. Larger shear deformation at the narrow region occurred basically due to the unstable thermo-mechanical behavior of the material. Due to the contact between tool tip and specimen, tremendous compressive stress was generated, which was higher than the strength of the specimen causing instability in plastic deformation during machining. Due to the occurrence of larger shear deformation, localized temperature was raised and the adiabatic shear band formed in dry cutting. However, in mist cooling condition, the adiabatic shear band was not so pronounced because of the diminishing localized temperature. Shear band formed easily in dry cutting because of significant deformation due to thermal softening of the workpiece, but in mist cooling it was not possible due to cooling and lubrication action of the coolant.

From SEM photographs shown in Figs. 13 and 14, it is presumed that at the highest level of cutting speed, i.e., 120 m/min in dry cutting condition, the adiabatic shear bands were more conspicuous when feed enhanced from 0.05 to 0.15 mm/rev because of the unavailability of sufficient time for heat removal from the specimen to the surroundings. Another conclusion can be drawn from the SEM images shown in Figs. 11 and 12 that the widths of the saw tooth were substantial in the dry cutting environment compared to mist cooling. As speed changed from 100 to 120 m/min, the shape of sawtooth on the chip surface was also differed. Wider saw tooth was formed on the chip surface in the dry cutting environment. Similar nature of saw tooth on chips was found at 0.05 and 0.15 mm/rev feed and 0.3 and 0.2 mm depth of cut. The transformation of chips from non-saw tooth to saw tooth type occurred when speed and feed altered from low level to high level.

Fig. 13 (a) and (b) Adiabatic shear band at feed 0.05 and 0.1 mm/rev with speed 120 m/min

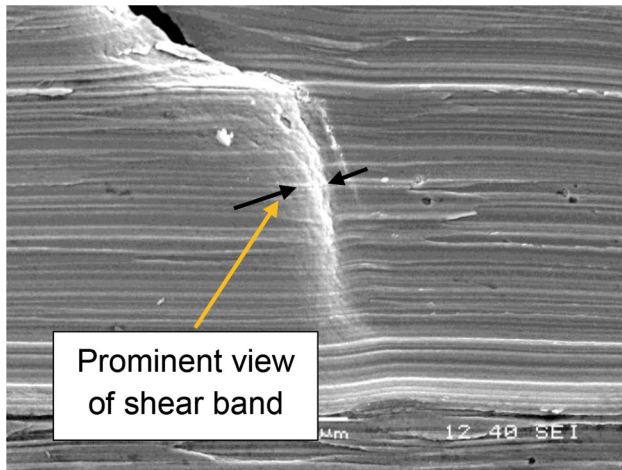
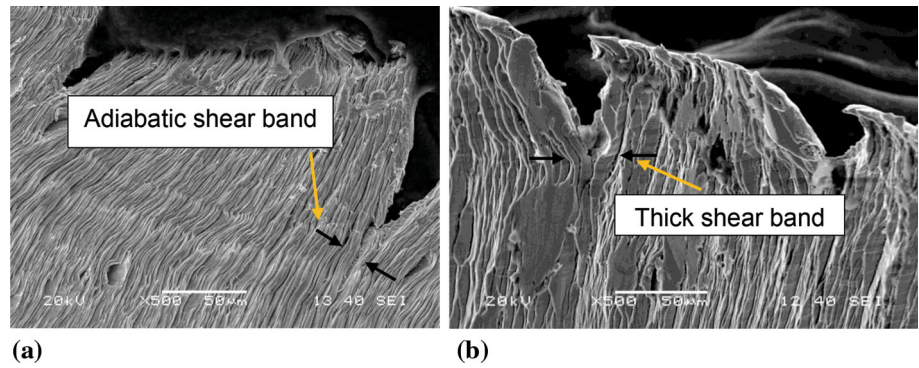


Fig. 14 Adiabatic shear band at speed 120 m/min with feed 0.15 mm/rev in dry cutting

Microhardness readings were in the range of 280–630 HV (28.2–56 HRC).

And from the ANOVA analysis, it can be concluded that feed was the governing parameter for the chip microhardness for both dry and mist cooling environments. Thus, when feed rate was upgraded, higher material removal rate was achieved which was subjected to high plastic deformation and temperature due to the enhancement of cutting force. Because of substantial plastic deformation and cutting temperature, hardening of chip occurred at the tool-chip interface. Figure 15 shows that the microhardness of chip increased as speed increased from 80 to 100 m/min in dry cutting, but it was slightly reduced in mist cooling and held almost constant for dry cutting condition for speed range from 100 to 120 m/min. This might be due to the increment of cutting temperature, which was prevailed by small time contact of insert and workpiece due to the higher cutting speed. Generation of a small amount of heat does not affect microstructural change and strain hardening of chips. As shown in Fig. 16, it was observed that higher value of chip microhardness was achieved in mist cooling

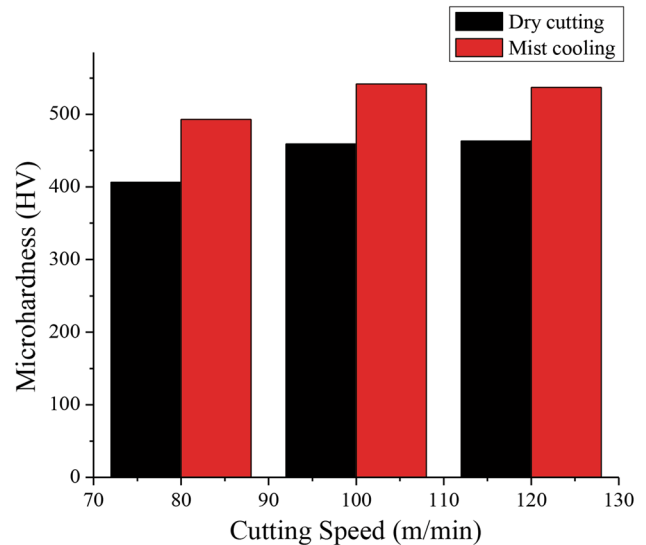


Fig. 15 Comparison of chip microhardness with cutting speed in both cutting conditions

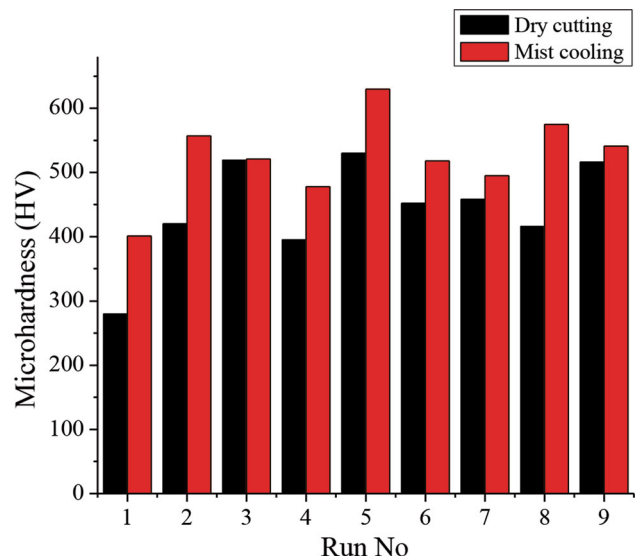


Fig. 16 Comparison of chip microhardness with experimental run in both cutting conditions

compared to dry cutting. Rapid cooling was achieved during mist cooling and for which untampered distorted martensite was observed at the microscopic level as shown in Fig. 17, which induced the hardness. Moreover, thick ridges, feed marks, embedded particles on chip surface and high strain marks were observed on chip surface in dry

condition as shown in Figs. 18b, 19b, 20 and 21, and these observations might be due to generation of high temperature. However, thin ridges, feed marks, no embedded particles and no strain marks were observed on chip surface during mist cooling as shown in Figs. 18 and 19a. The side flows of the chips were also found in dry cutting condition at higher speed, which are illustrated in Fig. 19b. This was prominently due to the higher working temperature in dry cutting condition. Overall good surface morphological characteristic of chip was observed in mist cooling compared to dry cutting [24, 25, 27].

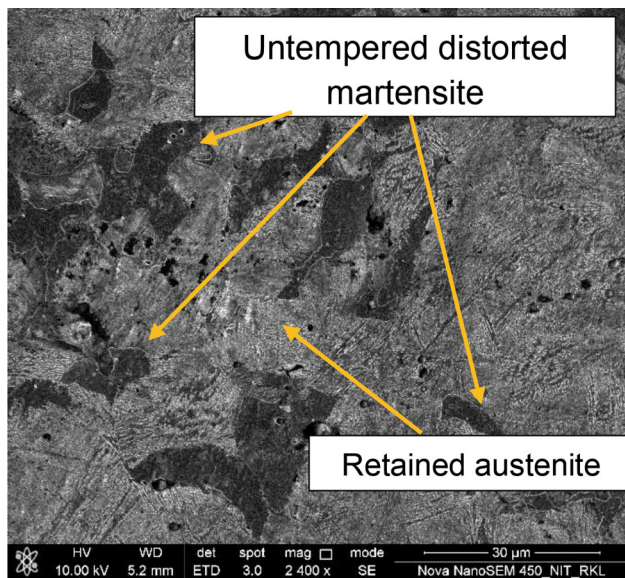


Fig. 17 Microstructure of hard turned steel sample with mist cooling

Surface Roughness Analysis

The arithmetical mean roughness parameter (Ra) of the test specimen was measured using (Taylor Hobson) surface roughness tester. The measuring and cutoff length were fixed as 4 and 0.8 mm, respectively. Prior to actual measurement, the instrument was calibrated properly. Measurement was taken around the circumference of the specimen and repeated three times at different locations of the machined area. Then, the mean value was considered as final. Compared to dry turning, least roughness values were observed in mist cooling condition as shown in Fig. 22, because in mist cooling, coolant penetrates in tool–chip interface and reduced the friction. In addition, a thin lubricating film formed between chip and tool, by which

Fig. 18 (a) and (b) Thin and thick ridges on chip surface during mist cooling and dry turning

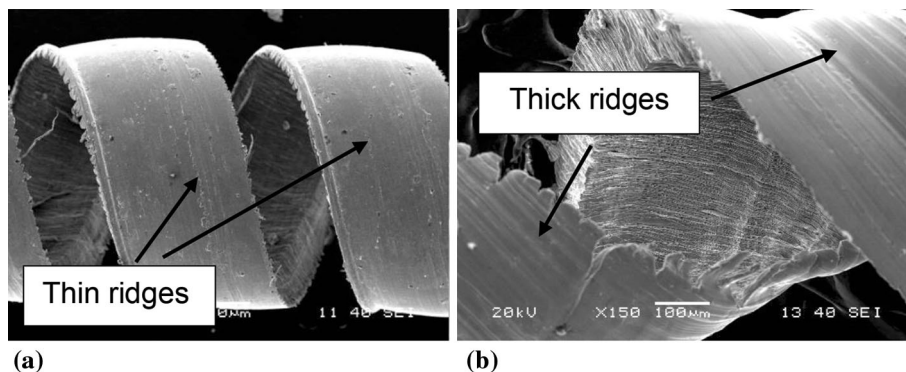
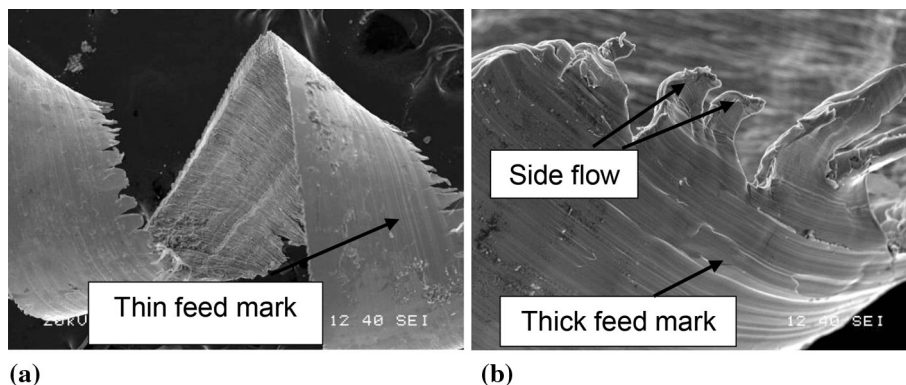


Fig. 19 (a) and (b) Thin and thick feed marks on chip surface during mist cooling and dry turning



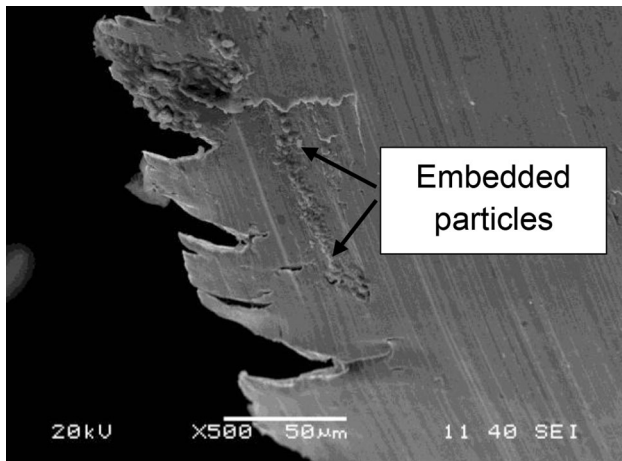


Fig. 20 Particles embedded on chip surface during dry cutting

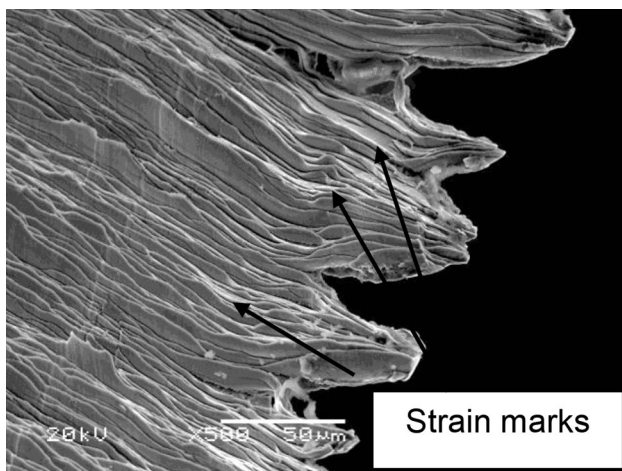


Fig. 21 High strain marks on chip surface during dry cutting

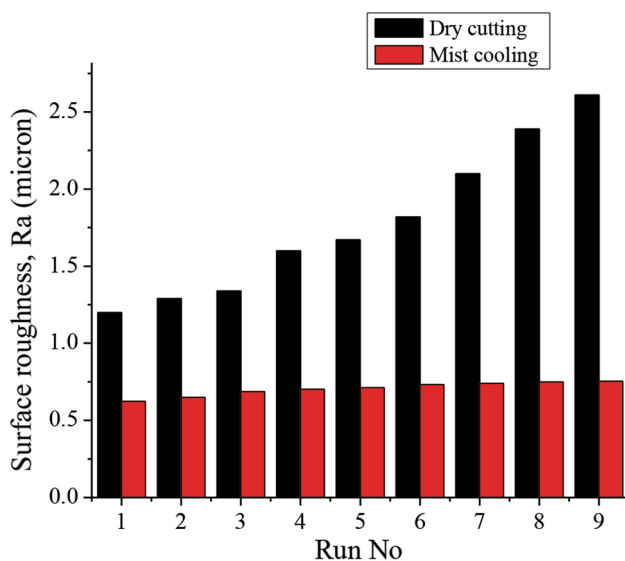


Fig. 22 Comparison of surface roughness with experimental run in both cutting conditions

the rubbing action of tool against the machined surface reduced. Also, less tool wear was observed in mist cooling compared to dry cutting, for which better surface finish in mist cooling condition was observed [1, 11, 14, 22, 26].

Conclusions

Conclusions drawn from the present experimental investigation are summarized as follows.

1. The performance of dry and mist cooled hard machining of alloy steel with coated cermet inserts was analyzed. The study confirmed that water-soluble coolant was a decent option for metal working fluid during hard turning of steel.
2. Chip microhardness and cutting force increased in mist cooling because of surface hardening.
3. Better tool life in terms of flank and crater wear was observed in mist cooling compared to dry cutting.
4. Chips with better morphological aspects were observed in mist cooled turning compared to dry turning.
5. Good surface finish was observed in mist cooled turning as compared to dry turning.

References

1. N.V.V.S. Sudheer et al., Investigation on influence of refrigerated air and high heat transfer rate MQL in turning of aluminium metal matrix composite, in *5th International & 26th All India Manufacturing Technology, Design and Research Conference (AIMTDR 2014)*, IIT Guwahati, Assam, India 12th–14th December 2014, pp. 454–1–454–6
2. S.A. Lawal et al., Experimental evaluation and optimization of flank wear during turning of AISI 4340 steel with coated carbide inserts using different cutting fluids. *J. Inst. Eng. India Ser. C* **96**(1), 21–28 (2015)
3. L.E.A. Sanchez et al., Cleaner machining through a tool holder with internal cooling, in *3rd International workshop Advances in Cleaner Production Sao Paulo-Brazil*, 18th–20th May 2011, pp. 1–10
4. A.U. Alkali et al., Influence of Cutting conditions on chip formation when turning ASSAB DF-3 hardened tool steel. *Int. J. Mater. Mech. Manuf.* **1**(1), 76–79 (2013)
5. A. Saini et al., Experimental estimation and optimization of process parameters under minimum quantity lubrication and dry turning of AISI- 4340 with different carbide inserts. *J. Mech. Sci. Technol.* **28**(6), 2307–2318 (2014)
6. A. Vardhaman et al., Examining the role of cutting fluids in machining AISI 1040 steel using Taungsten carbide insert under minimal quantity lubrication condition, in *3rd International Conference on Advances in Engineering Sciences & Applied Mathematics (ICAESAM 2015)* 23–24th March 2015, pp. 80–83
7. M.H.S. Elmunafi et al., Tool life of coated carbide cutting tool when turning hardened stainless steel under minimum quantity lubricant using castor oil, in *2nd International Materials, Industrial, and Manufacturing Engineering Conference, MIMEC2015*,

- Bali Indonesia, Procedia Manufacturing, 4–6th February 2015, pp. 563–567
8. D.A. Stephenson et al., Rough turning Inconel 750 with supercritical CO₂-based minimum quantity lubrication. *J. Mater. Process. Technol.* **214**(3), 673–680 (2014)
 9. P.S.C. Bose et al., Role of MQL and nano fluids on the machining of NICROFER C263, in *5th International & 26th All India Manufacturing Technology, Design and Research Conference (AIMTDR 2014)*, IIT Guwahati Assam, India, 12th–14th December 2014, pp. 363-1–363-5
 10. P.V. Krishna et al., Experimental investigation on the performance of nanoboric acid suspensions in SAE-40 and coconut oil during turning of AISI 1040 steel. *Int. J. Mach. Tools Manuf.* **50**(10), 911–916 (2010)
 11. P. Netake, S. Chinchankar, Hard turning under minimum quantity lubrication: modelling of cutting force and surface roughness. *J. Adv. Eng. Res.* **2**(1), 17–22 (2015)
 12. G.S. Goindi et al., Investigation of ionic liquids as metal working fluids in minimum quantity lubrication machining of AISI 1045 Steel, in *5th International & 26th All India Manufacturing Technology, Design and Research Conference (AIMTDR 2014)*, IIT Guwahati Assam, India, 12th–14th December 2014, pp. 277-1–277-6
 13. D.K. Sharma, U.S. Dixit, A comparison of dry and air-cooled turning of grey cast iron with mixed oxide ceramic tool. *J. Mater. Process. Technol.* **190**(1–3), 160–172 (2007)
 14. M.M.A. Khan et al., Effects of minimum quantity lubrication on turning AISI 9310 alloy steel using vegetable oil-based cutting fluid. *J. Mater. Process. Technol.* **209**(15–16), 5573–5583 (2009)
 15. S.J. Ojolo et al., Experimental determination of the effects of some straight biological oils on cutting force during cylindrical turning. *Rev. Mater.* **13**(4), 650–663 (2008)
 16. N.R. Dhar et al., The influence of minimum quantity of lubrication (MQL) on cutting temperature, chip and dimensional accuracy in turning AISI-1040 steel. *J. Mater. Process. Technol.* **171**(1), 93–99 (2006)
 17. A.E. Diniz et al., Influence of refrigeration/lubrication condition on SAE 52100 hardened steel turning at several cutting speeds. *Int. J. Mach. Tools Manuf.* **43**(3), 317–326 (2003)
 18. S.S. Gill et al., Wear behaviour of cryogenically treated tungsten carbide inserts under dry and wet turning conditions. *Int. J. Mach. Tools Manuf.* **49**(3–4), 256–260 (2009)
 19. A. Attanasio et al., Minimal quantity lubrication in turning: effect on tool wear. *Wear* **260**(3), 333–338 (2006)
 20. O. Cakir et al., Comparison of gases applications to wet and dry cutting in turning. *J. Mater. Process. Technol.* **153–154**, 35–41 (2004)
 21. P. Selopal, O.S. Bhatia, Lubrication: a review. *Int. J. Adv. Res. Ideas Innov. Technol.* **1**(2), 1–7 (2015)
 22. G. Singh et al., Experimental investigations of vegetable & mineral oil performance during machining of En-31 steel with minimum quantity lubrication. *Int. J. Res. Eng. Technol.* **2**(6), 1030–1037 (2013)
 23. R.W. Maruda et al., Tool wear characterizations in finish turning of AISI 1045 carbon steel for MQCL conditions. *Wear* **372–373**, 54–67 (2017)
 24. R.W. Maruda et al., The influence of the cooling conditions on the cutting tool wear and the chip formation mechanism. *J. Manuf. Process.* **24**, 107–115 (2016)
 25. R.W. Maruda, E. Feldshtein, Some features of ecological finish turning of low carbon steels. *Achiev. Mech. Technol. Autom.* **33**(2), 13–23 (2013)
 26. R.W. Maruda et al., Effect of anti-wear additive on cutting tool and surface layer of workpiece state under MQCL conditions. *Tech. Gaz.* **22**(5), 1219–1223 (2015)
 27. R.W. Maruda et al., Influence of cooling conditions on the machining process under MQCL and MQL conditions. *Tech. Gaz.* **22**(4), 965–970 (2015)